Exploring the Earth

NORSAR Scientific Report No.2-2014

Semiannual Technical Summary

1 July – 31 December 2014

Tormod Kværna (Ed.)

Kjeller, August 2015

NORSAR

6 Technical Reports / Papers Published

6.1 3-D Crustal Model for Southern Norway

6.1.1 Introduction

The presented study is a part of the Norwegian National Seismological Network (NNSN) project carried out by the University of Bergen (UiB) in cooperation with NORSAR. In this study we aim to obtain a 3-D crustal model of P and S waves for Norway. Here we present our results obtained for the southern part of Norway limited to 56-65° N latitude and 2-14° E longitude.

Development of the 3-D velocity model was divided into two steps:

1) To obtain the optimal 1-D velocity model of the Earth's crust in the study area. The model was obtained using the VELEST program (Kissling et al., 1994) which is implemented into the SEISAN program package (Ottemoller et al., 2014). The VELEST was modified at NORSAR implementing station naming of five symbols and transformation for a spherical earth. The obtained model is used as a reference velocity model for development of the 3-D model.

2) To obtain the 3-D velocity model. The model was obtained using the FMTOMO program (Rawlinson and Sambridge, 2005).

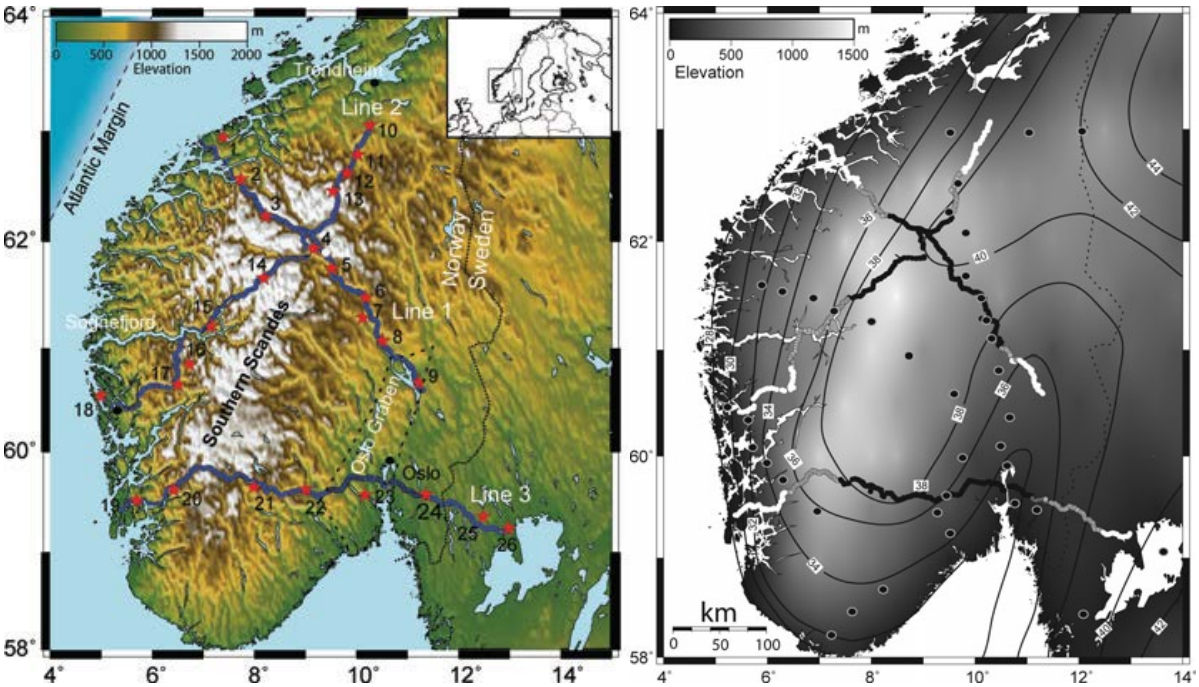

Fig. 6.1.1 (After Stratford et al., 2009) (Left panel) Study area of the Magnus-Rex project. Red stars indicate locations of shots, blue dots indicate the seismic stations. The shot lines 1, 2 and 3 marked in blue. Insert: map of northern Europe showing the study area. (Right panel) New Moho map for southern Norway. Labelled contours represent Moho depth in km.

The obtained 1-D and 3-D velocity models may improve the location results of the local seismic events originating in southern Norway.

6.1.2 Previous studies

The geological – tectonic conditions in Norway are very complicated. The territory of Norway experienced a number of different tectonic regimes: uplift and subsidence (Lidmar-Bergstrøm et al., 2000), folding and faulting which resulted in dislocation of nappes (Roberts and Gee, 1985). After the Caledonian orogeny the region experienced an extensional regime (Andersen, 1998). The uplift processes due to erosion (Faleide et al., 2002) and postglacial rebound (Balling, 1980) are still present.

Some studies of the Earth's crust in the southern part of Norway have previously been carried out. The early efforts to define depth of the Moho boundary were performed using data of refraction profiling. The results showed that the crust is about 38 km thick beneath the mountains (Sellevoll and Warrick, 1971), while more recent studies of receiver functions estimate the Moho to about 43 km depth in this part. In 2007 there was carried out a seismic refraction experiment Magnus-Rex (Stratford et al., 2009), during which three nearly 400 km long seismic lines were deployed in southern Norway. The results obtained from the studies of Magnus-Rex data indicate Moho depth variations from about 30 to about 40 km (Figure 6.1.1) along the indicated profiles in Figure 6.1.2. This result is quite consistent with the recent receiver function studies by Kolstrup (2015) (Figure 6.1.3).

6.1.3 Study area and dataset

The study area is limited to 58-65° N latitude and 4-14° E longitude. We used seismological data recorded by seismic stations deployed in southern Norway during different projects (Figure 6.1.1). The compiled dataset contains 175 seismic events (Table 6.1.2):

1) 47 events from the original UiB seismological catalog (year 2009-2013). The events were re-picked and relocated at NORSAR using the same velocity model which is used by the UiB;

2) 72 events from the MAGNUS project (year 2007-2008). The data was analyzed at the UiB;

3) 32 events from NORSAR seismological bulletins (year 2014);

4) 24 explosions from the Magnus-Rex project; the data was analyzed at NORSAR.

Statistics for inversion with the VELEST program:

1) 175 local seismic events: 151 events (both natural and man-made quarry blasts) and 24 explosions from the Magnus-Rex project;

2) 105 seismic stations;

3) 4347 phase readings: 2922 P wave arrivals and 1425 S wave arrivals.

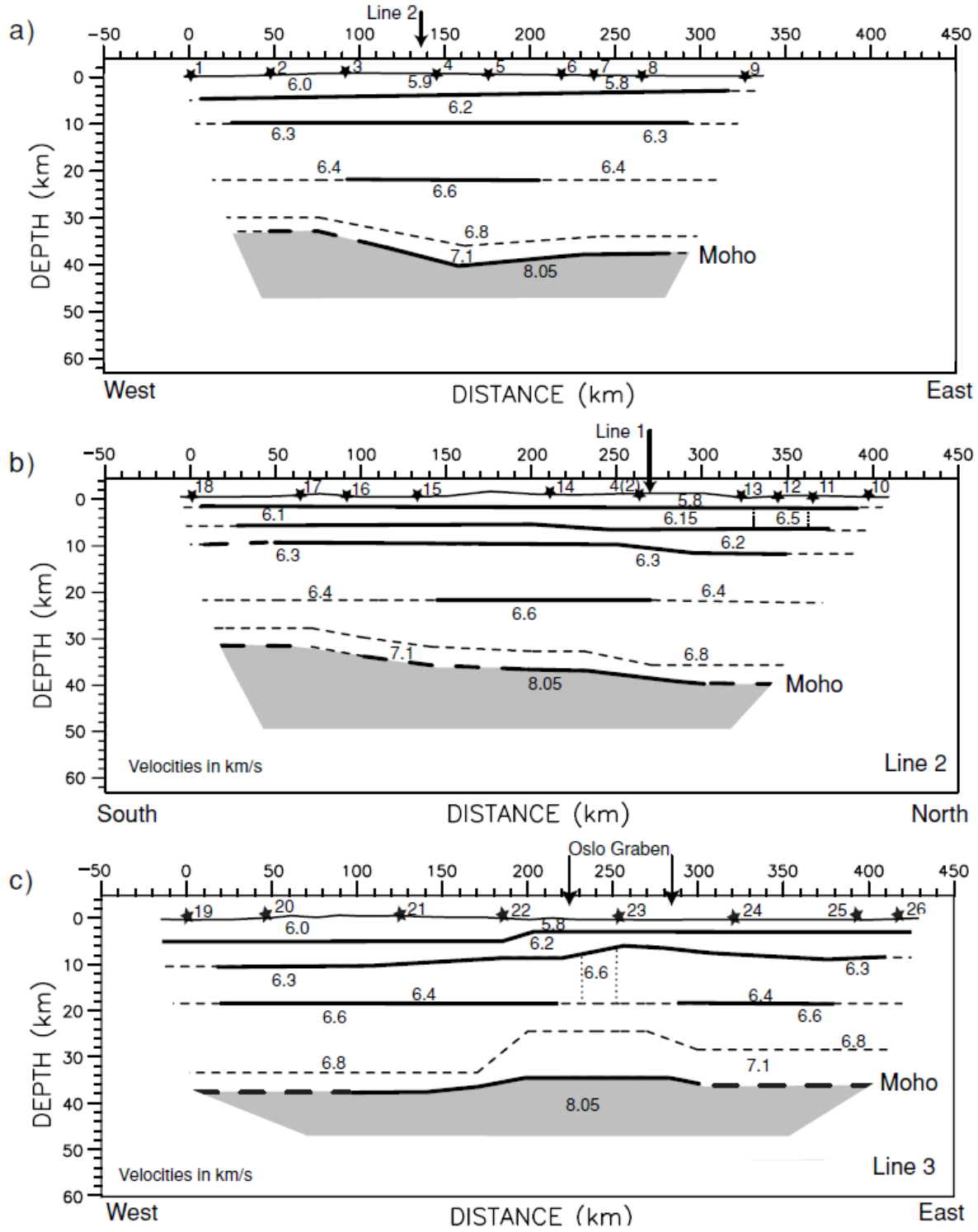

Fig. 6.1.2 (After Stratford et al., 2009) Forward modelling ray tracing solution for lines (a) 1, (b) 2 and (c) 3. The cross point between lines 1 and 2 is marked on the seismic models with labelled arrows. The surface expression of the Oslo Graben is marked on line 3.

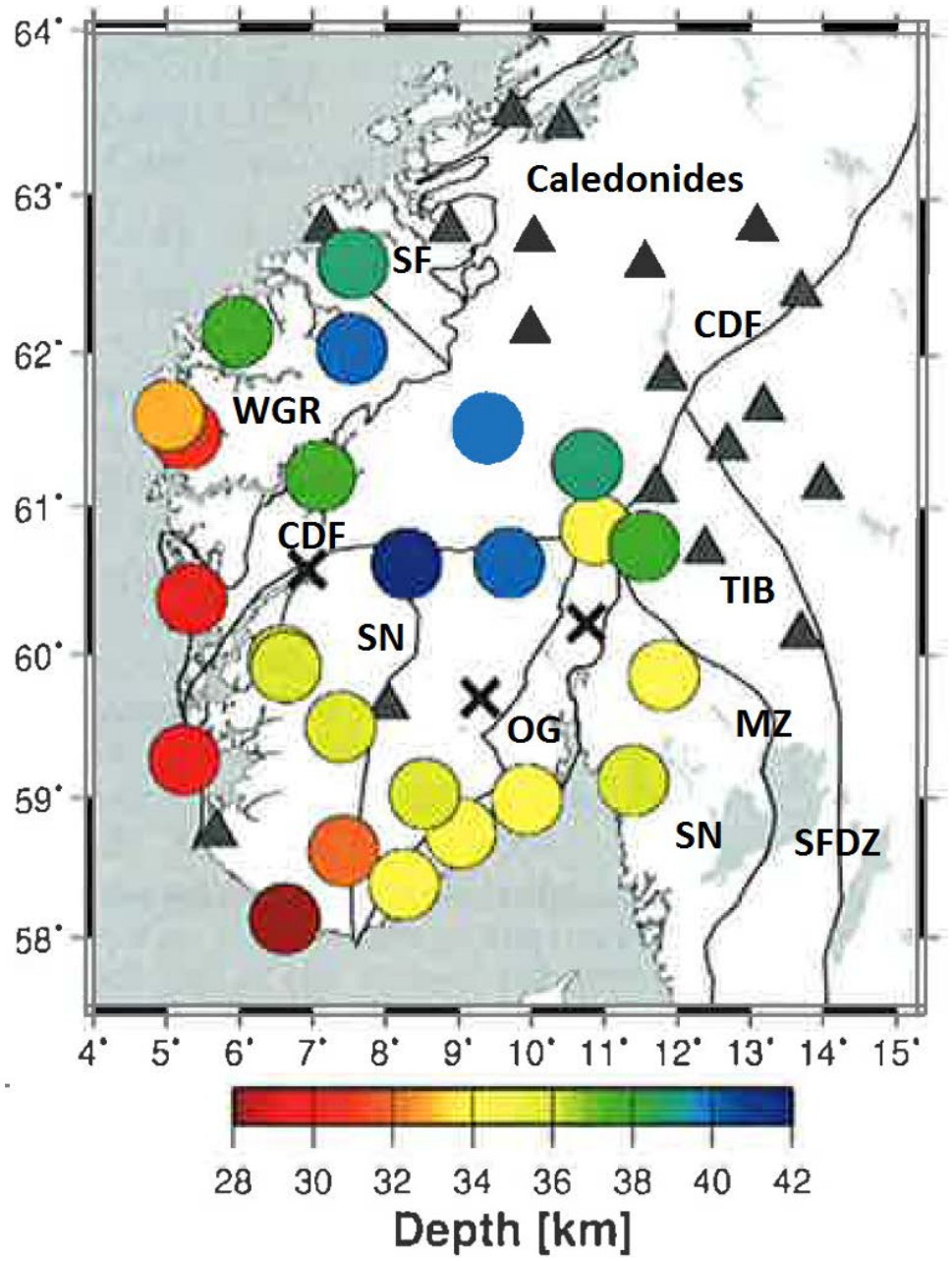

Fig. 6.1.3 (After Kolstrup, 2015) The Moho map. Colored circles indicate the Moho depths, grey triangles indicate locations of stations with gradual crust-mantle transition, black crosses indicate locations of stations where joint inversion was not performed, and black lines depict main geological units and boundaries: CDF, Caledonian front; MZ, Mylonite Zone, OG, Oslo Graben; SN, Sveconorwegian; SF, Sveconorwegian front; SFDZ, Sveconorwegian Frontal Deformation Zone, TIB. Transscandinavian Igneous Belt, WGR, Western Gneiss Region.

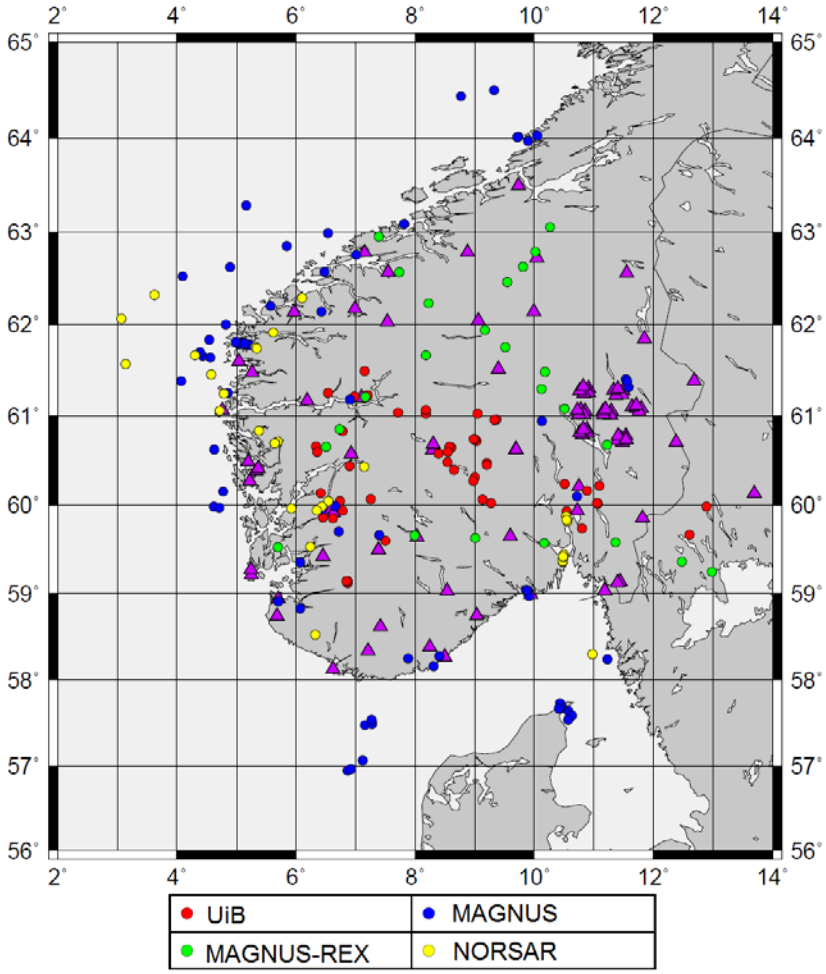

Fig. 6.1.4 Distribution of events used for development of the optimal 1-D velocity model for southern Norway. Triangles – seismic stations, circles – epicenters of seismic events: red – relocated events from the UiB catalog, blue – events from the MAGNUS project, green – explosions of the Magnus-REX project, yellow – events from the NORSAR catalog.

6.1.4 Development of the optimal 1-D velocity model

We performed inversions with the VELEST program using different settings, and defined optimal parameters for our dataset. We found that values of velocity and depth adjustments are, respectively, 0.2 km/s and 5.0 km for each iteration. We inverted for both P and S waves simultaneously, keeping the Vp/Vs ration equal to 1.74. We did not investigate the influence of different damping values and used the default values: 0.01 for epicenter coordinates, hypocenter depth and station corrections, and 1.00 for velocity values. The inversions with the VELEST program were performed in simultaneous mode. During each iteration (we performed 5 iterations) an inversion for all hypocenters and velocity model, including station corrections, was performed.

The input 1-D velocity models for both P and S waves were parameterized from the surface down to 80 km depth. Three different input velocity models were tested (Figure 6.1.5):

- Model ***b***: is the velocity model used by the UiB to locate seismic events in the southern part of Norway.

- Model ***mt***: is an averaged velocity model compiled from the results by Stratford and Thybo (2011) obtained from the MAGNUS project.

- Model ***m2***: is a modified ***mt*** model (i.e. fewer layers).

We analyzed the inversion results obtained with the different velocity models ***b***, ***mt*** and ***m2*** to define which one of them is the most suitable. We analyzed the data variance and final RMS values (Figure 6.1.6), distribution of the RMS values (Figure 6.1.7), hypocenter depth (Figure 6.1.8), and geographical distribution of hypocenter depths (Figure 6.1.9) and RMS values (Figure 6.1.10) of the relocated events. From the analysis we concluded that an optimal 1-D velocity model for southern Norway is the output model from the VELEST inversion with the input ***m2*** model (Table 6.1.1).

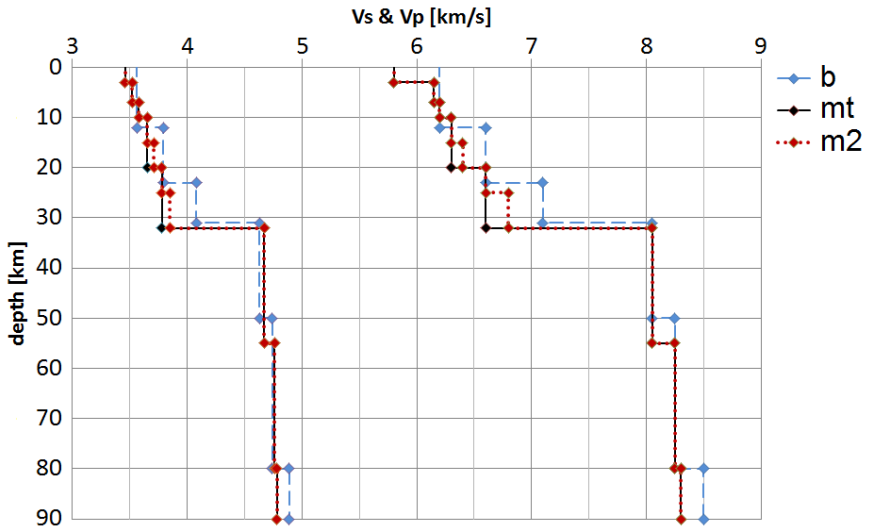

Fig. 6.1.5 Tested input velocity models b, mt and m2 for S waves (left curves) and P waves (right curves).

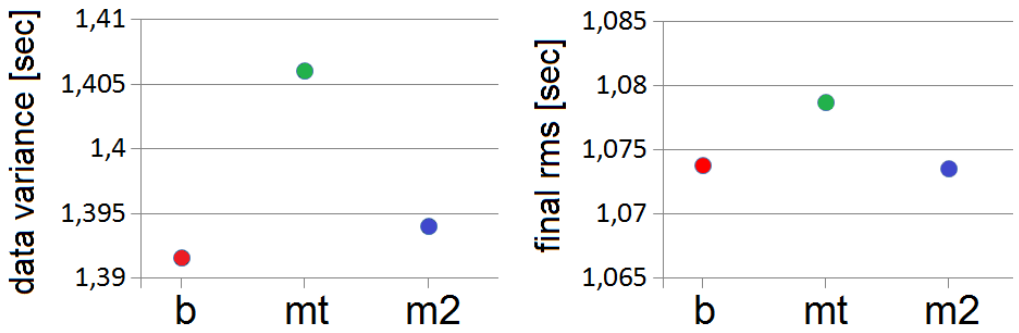

Fig. 6.1.6 Data variance and final RMS values after the VELEST inversions with different velocity models. Models are indicated on the abscissa.

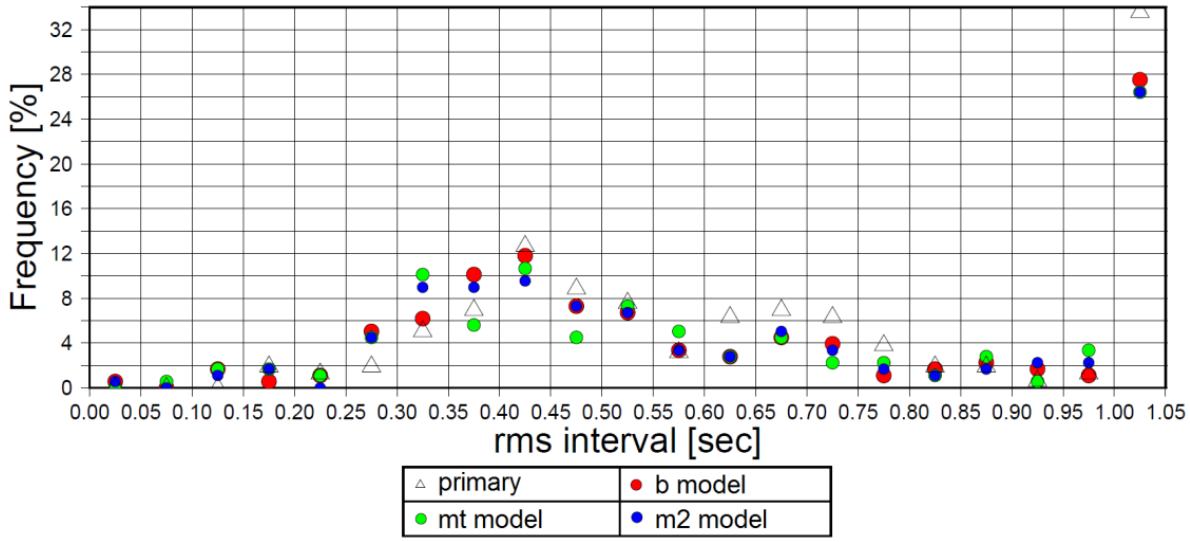

*Fig. 6.1.7 Distribution of the RMS values of the primary dataset (triangles) (from the original UiB seismological catalogs) and the output velocity models obtained using different input velocity models **b**, **mt** and **m2** (colorful circles).*

Table 6.1.1 Optimal 1-D velocity model for southern Norway. Seismic velocities of P and S waves are expressed in km/s, depth is in km. Moho boundary indicated by an arrow.

depth	Vp	Vs	Vp/Vs	
0.00	5.99	3.46	1.731	
3.00	6.18	3.50	1.765	
7.00	6.34	3.53	1.796	
10.00	6.46	3.70	1.746	
15.00	6.47	3.70	1.748	
20.00	6.52	3.74	1.743	
25.00	6.52	3.74	1.743	
32.00	7.76	4.35	1.784	← Moho
55.00	8.18	4.77	1.715	
80.00	8.30	4.78	1.736	

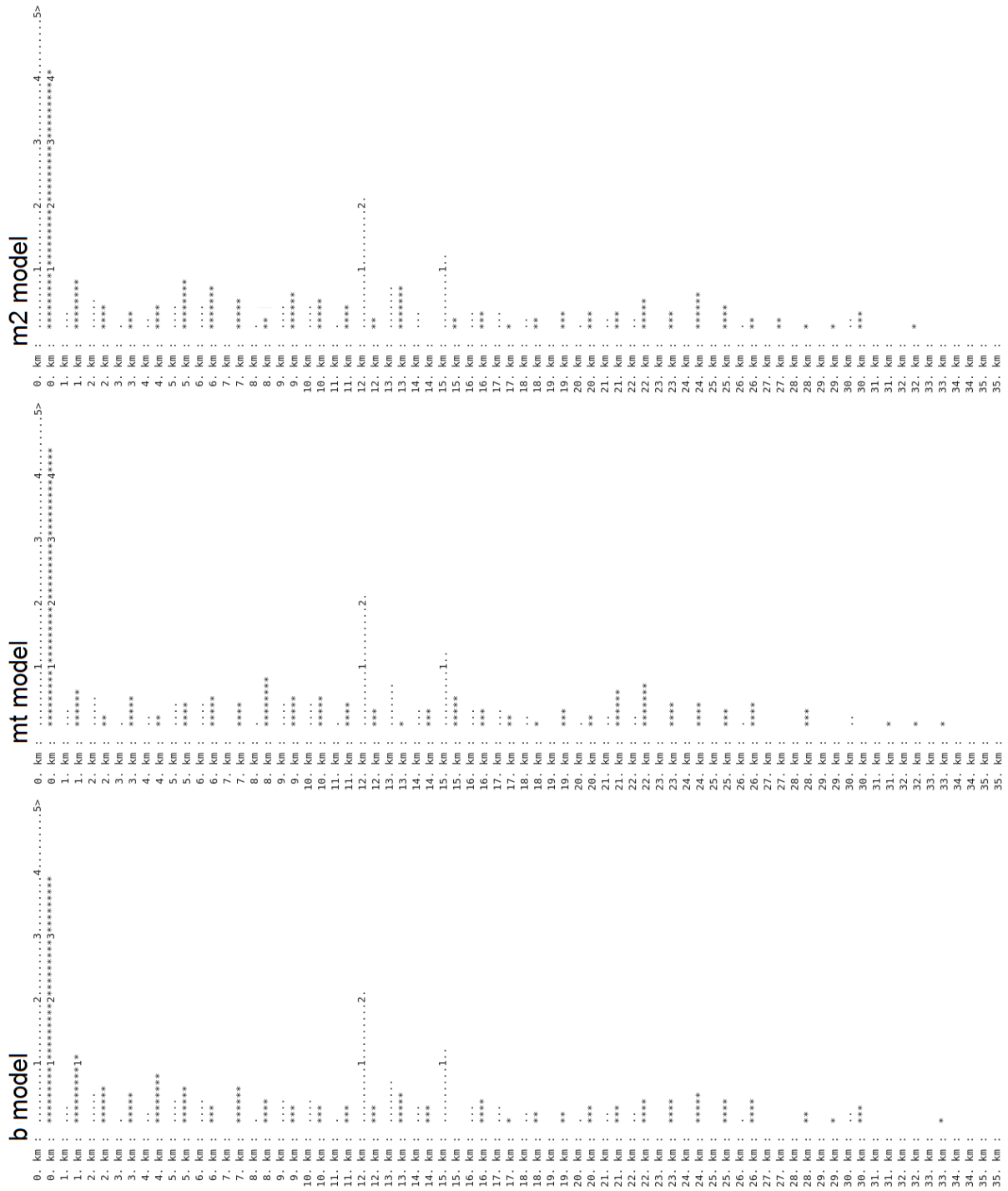

*Fig. 6.1.8 Distribution of depths of hypocenters after the VELEST inversions with different input velocity models **b**, **mt** and **m2**. Dots – primary depth values, stars – output hypocenter depths.*

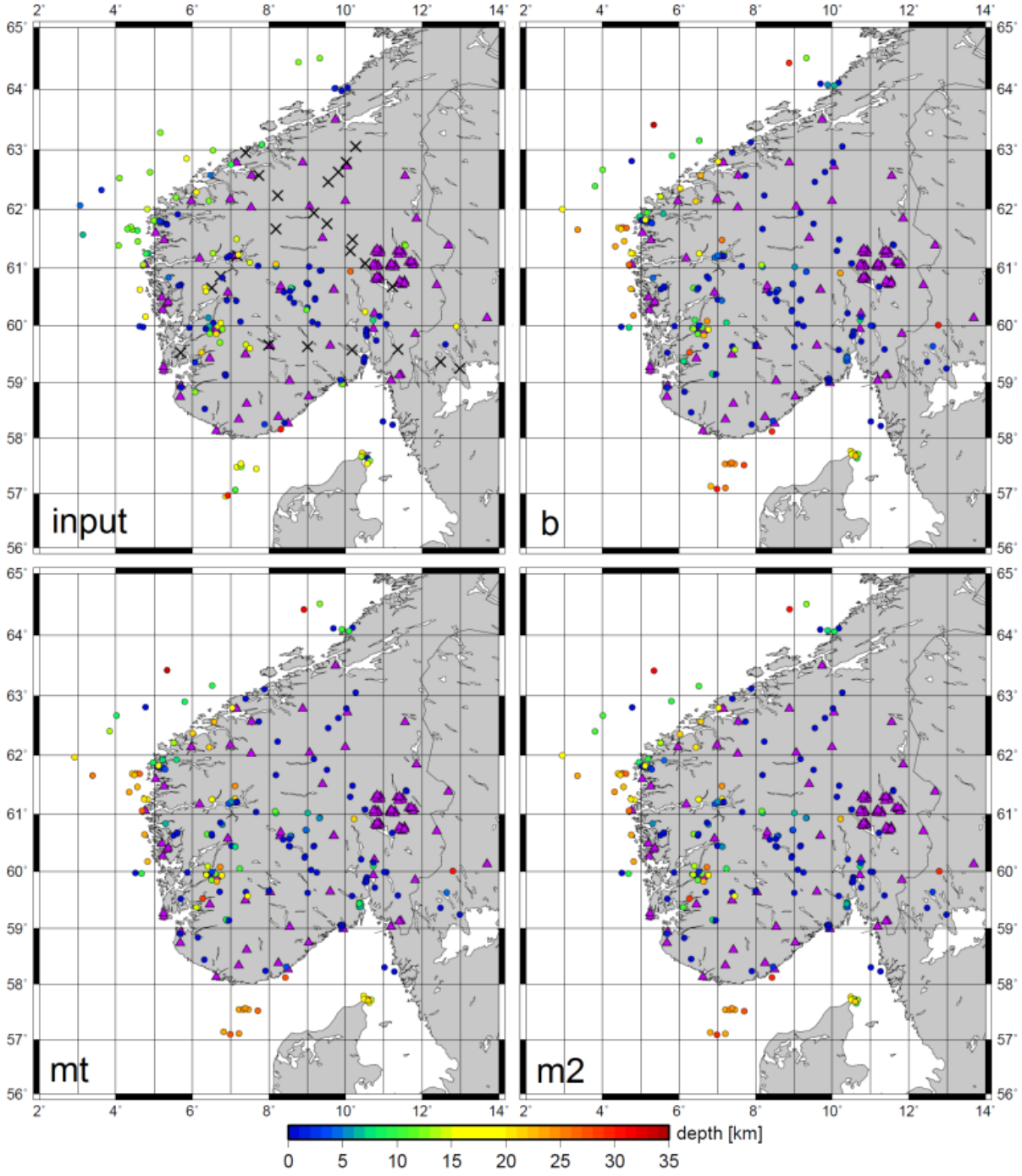

Fig. 6.1.9 Map of locations of events with indicated hypocenter depths for input and output of different models. x – explosions of the Magnus-REX project blasted close to the surface, circles – other seismic events. Depth of the explosions were fixed during the inversion.

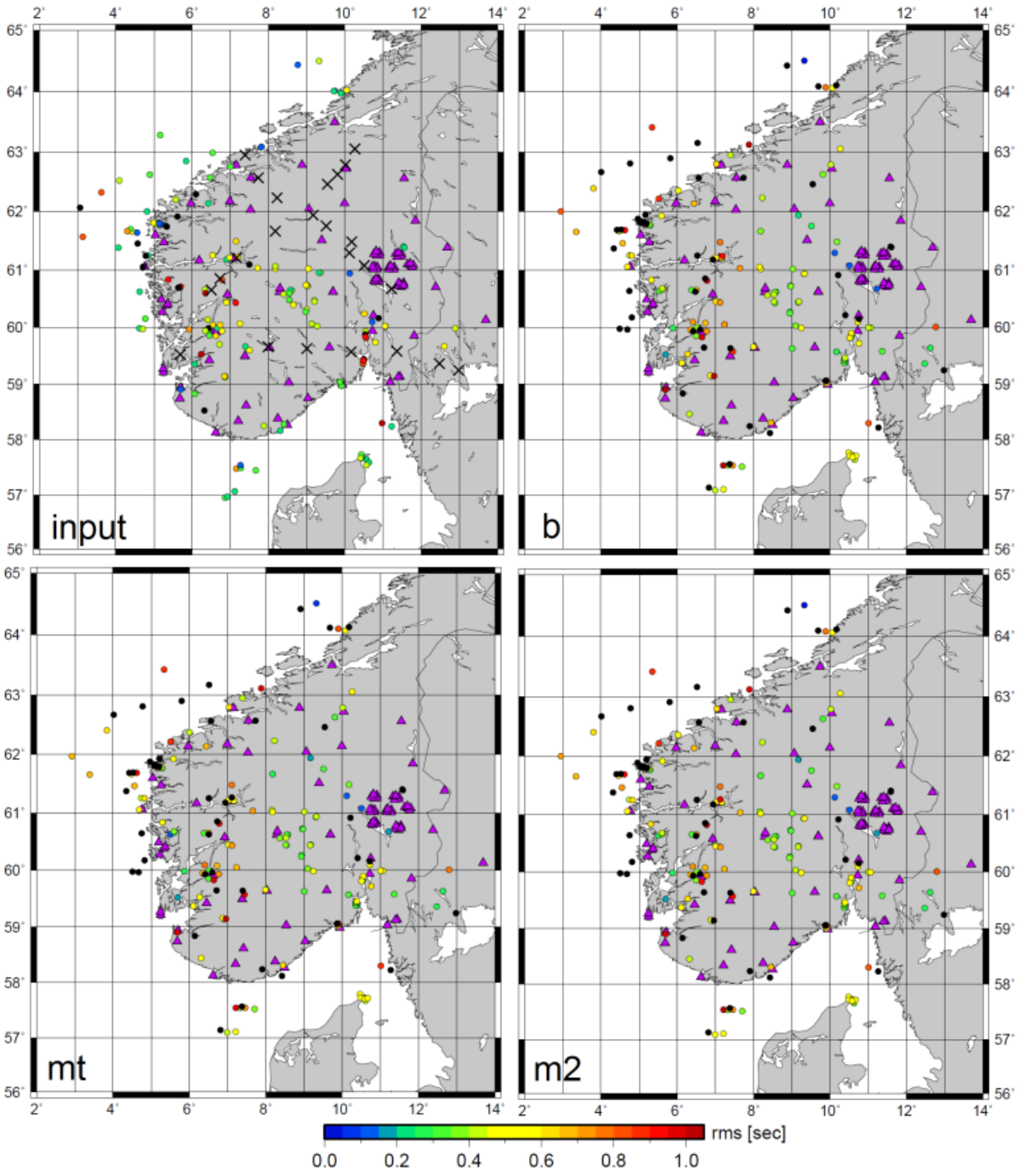

Fig. 6.1.10 Map of locations of events with indicated RMS value of the location for input and output of different models. x – explosions of the Magnus-REX project blasted close to the surface, circles – seismic events.

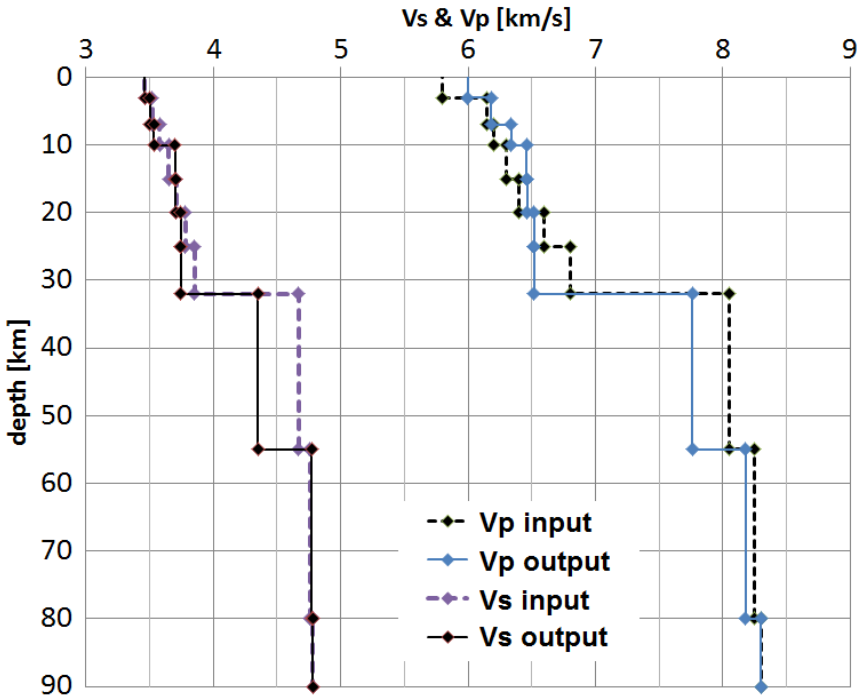

Fig. 6.1.11 Curves of m2 input and output velocity models for S (left) and P waves (right). The m2 output velocity model is regarded as an optimal 1-D velocity model for the southern part of Norway.

6.1.5 Development of the 3-D velocity model

6.1.5.1 Model parameterization

We defined the study area to 56-65° N latitude and 2-14° E longitude, and parameterized the model with two layers extending from the surface down to 80 km deep. The size of the model cells was selected taking into account the frequency content of the seismic signals and distribution of sources and receivers within the area. The size of the model cell is 0.9 degree in longitude and 0.7 degree in latitude, while the vertical spacing between the grid nodes is about 3 km in the upper layer and 4 km in the lower layer.

The 1-D velocity model (Figure 6.1.11) obtained with the VELEST program was used as a reference velocity model for further studies using the FMTOMO program. Before implementing the velocity model into the FMTOMO program, it was modified according to the studies by Stratford et al. (2009) and Stratford and Thybo (2011), and was transformed into a velocity model with two layers of gradient velocities increasing with depth (Figure 6.1.12). The upper layer extends from the surface to 32.1 km depth, and Vp in the layer gradually increases from 6.0 to 7.1 km/s, while the lower layer extends from 32.1 km to 80.0 km depth, and Vp in the layer changes from 8.05 to 8.30 km/s.

In the study we used damping of 1.0 for the velocity inversion and 0.1 for interface inversion. We did not investigate the influence of using different damping values.

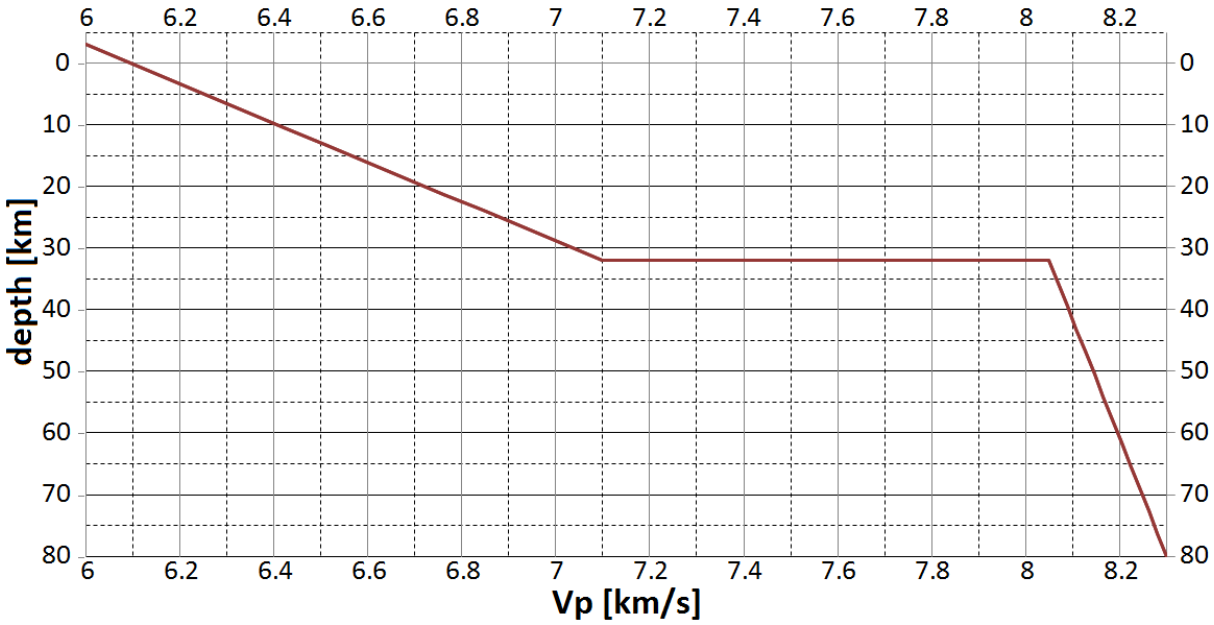

Fig. 6.1.12 Reference 1-D velocity model for southern Norway used to perform inversions with the FMTOMO program.

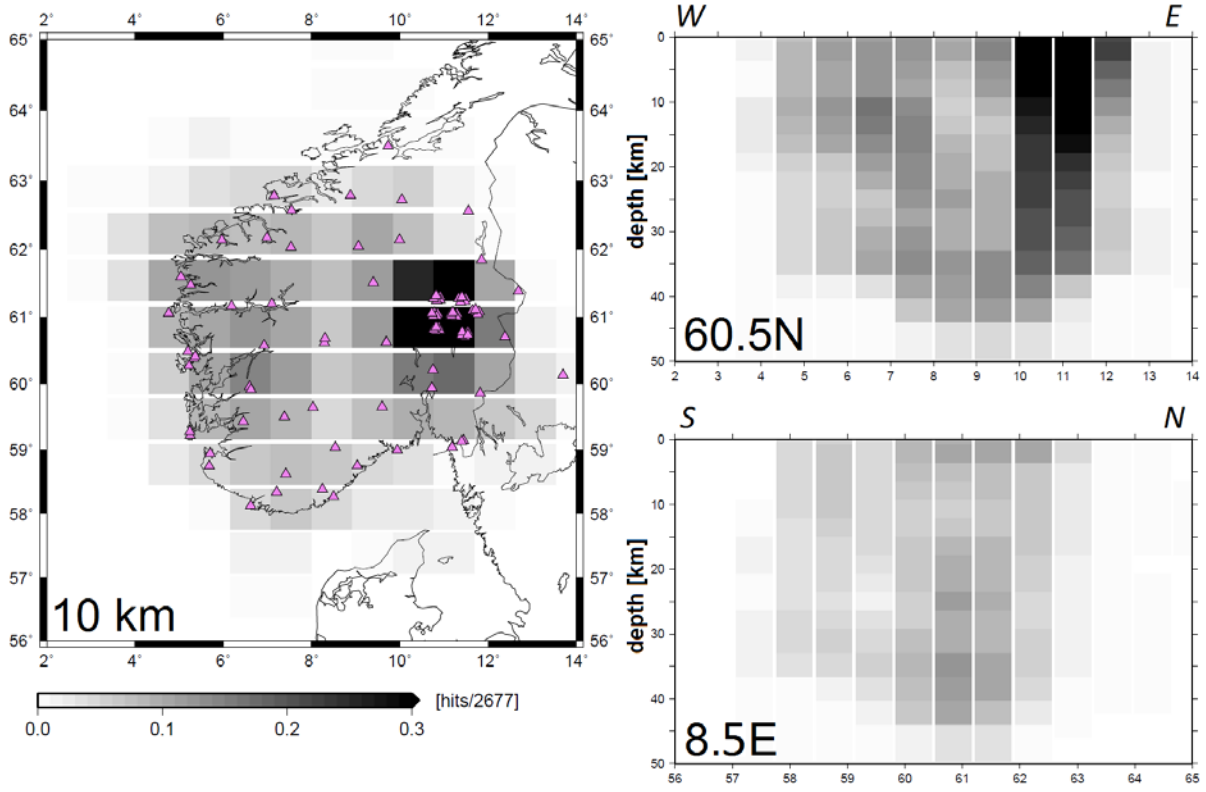

Fig. 6.1.13 Horizontal and two vertical perpendicular slices of the hit matrix in the study volume. The values are normalized to the total number of the rays.

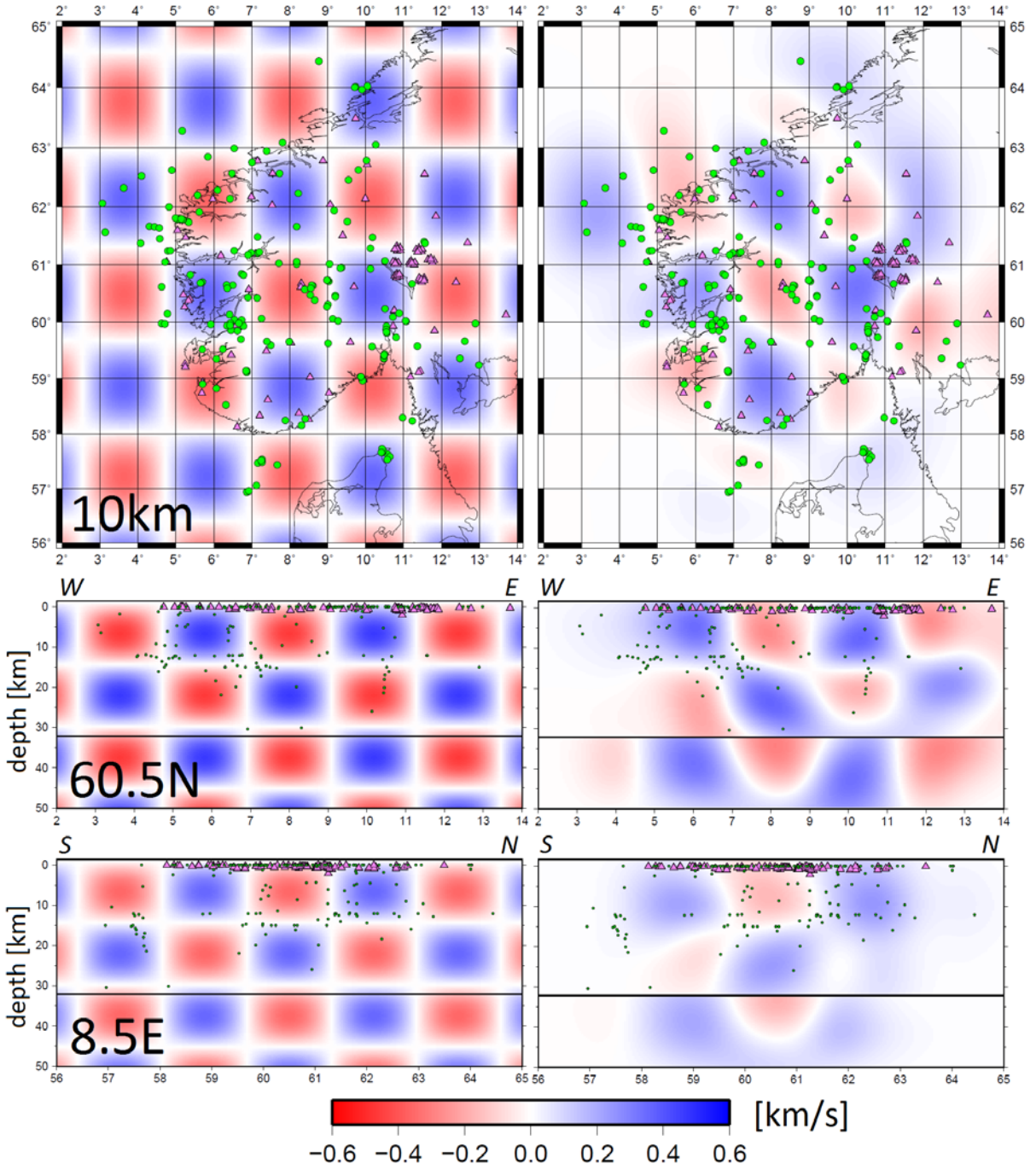

Fig. 6.1.14 Checkerboard test. (Left) Input checkerboard velocity model with synthetic blocks of ± 0.6 km/s velocity variations compared to the reference velocity model, and (right) the resolved model.

6.1.5.2 Resolution

Before analyzing the results with the real data it is very important to assess resolution. In this study we applied two methods: 1) the synthetic checkerboard test, and 2) the hit matrix, in order to obtain the ray coverage and define areas with good and poor resolution capabilities. The hit matrix shows how many rays cross the particular cell (Figure 6.1.13). However, the hit matrix method alone does not show the ray crossing, thus we need additional tools, such as checkerboard test, to define the regions, which could be confidently resolved with the current configuration of sources and receivers.

We used a synthetic checkerboard model (Figure 6.1.14) with synthetic blocks embracing two cells in all directions with alternating velocity variations of ±0.6 km/s compared to the reference velocity model. The inversion results with the checkerboard model show that the best resolved part of the study area is the central part down to about 35-40 km depth, while going to the outskirts the resolution depth decreases (Figure 6.1.14).

6.1.5.3 Inversion results

We performed an inversion with the real dataset and as a result we obtained a distribution of velocity variations within the study volume (Figure 6.1.15). In the inversion we introduced a constant Moho boundary at 32.1 km depth. The inversion was performed simultaneously for P wave perturbations and the Moho interface.

The model for seismic S waves can be obtained using the Vp/Vs ratios obtained from the VELEST program. The ratios are indicated in Table 6.1.1.

In the study we obtained a distribution of velocity variations within the study area from surface down to about 35-40 km depth (Figure 6.1.13, 6.1.14, 6.1.15). The amplitudes of velocity variations depend on the damping value, model grid, reference velocity model and errors in the dataset (i.e. phase picking). Our results show that P wave velocities in the areas with reasonable resolution vary about ±0.4 km/s compared to the reference velocity model. The higher velocity values are observed in the middle part of the study area, i.e. beneath the mountain plateau of southern Norway. We indicate that the deepest Moho boundary in this part is reaching 34-35 km, while the shallowest Moho of 31 km is found slightly to the north of the Oslo Graben. The shallow Moho depth is also found beneath the SW part of the study area, along the coast. Stratford et al. (2011) indicate a slightly deeper Moho boundary in the study area compared to our study. Their study indicates the deepest Moho at about 38-39 km beneath the mountain plateau and the shallowest Moho at about 32 km depth along the SW coast, while the study by Kolstrup (2015) indicates a variation of the Moho depth from about 40 km in the central part to about 28 km on the SW coast.

Oslo Graben is in many studies characterized as a pronounced tectonic structure (e.g. Stratford et al., 2011). Our results for the Oslo Graben indicate lower velocity values compared to the reference velocity model in the upper and the lower parts of the model, and slightly higher values between 10 and 15 km depth. Stratford et al. (2011) report on a higher velocity body beneath the Oslo Graben from 10 to 20 km. Stratford et al. (2011) estimate a Moho boundary at about 34 km depth, while we observe it at about 31 km, however, our checkerboard test indicates quite poor resolution at this depth.

In the southernmost part, most likely, we recognize a continuation of the most significant tectonic boundary in Europe, the Trans-European Suture Zone (TESZ); its northern part is called the Sorgenfrei–Tornquist Zone (STZ). The STZ in our results could be related with the higher velocity area extending downwards from at least 10 km. However, the resolution in this part is relatively poor.

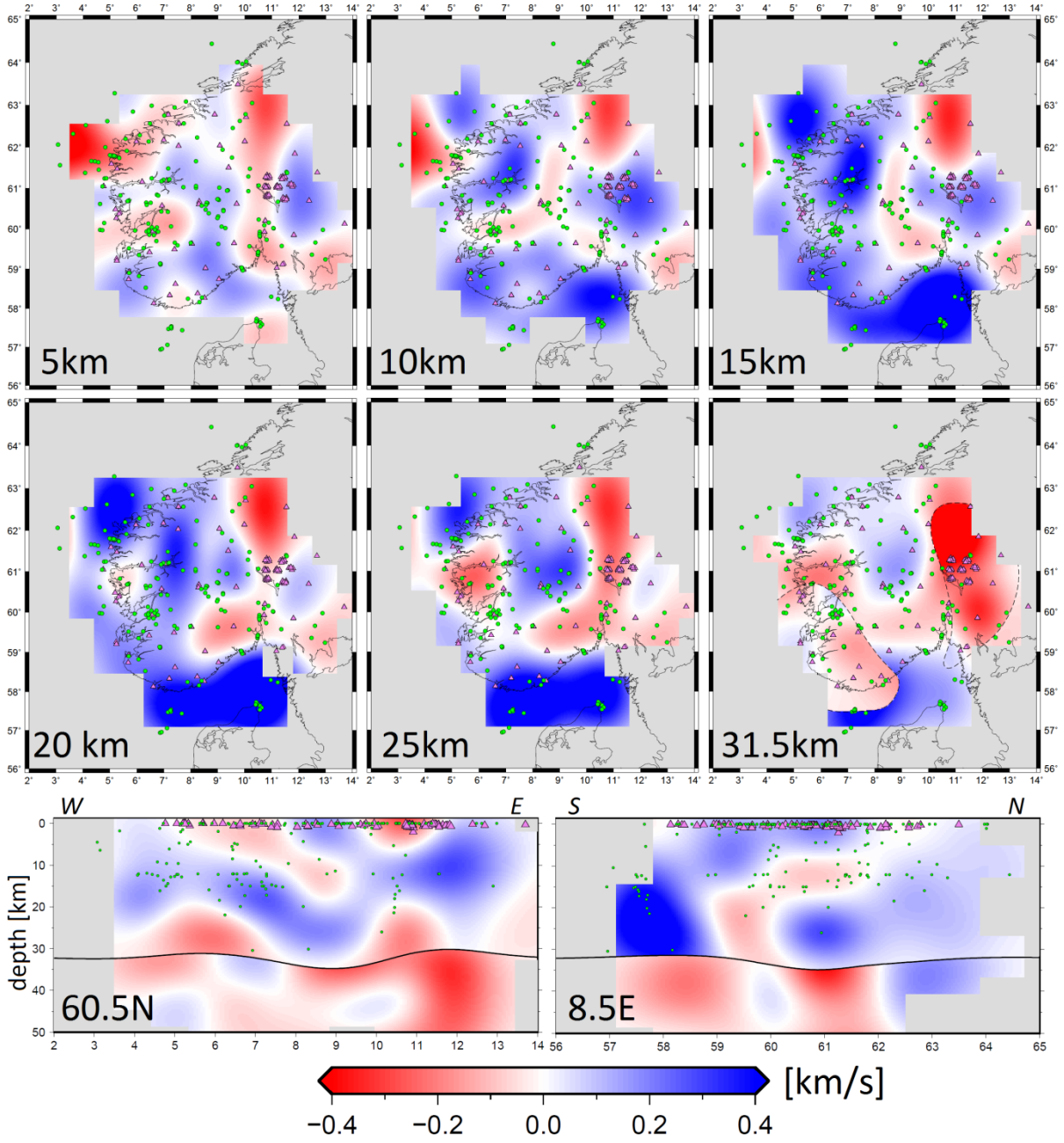

Fig. 6.1.15 Inversion results with the real dataset. Horizontal and vertical slices of the target volume are shown. Blue and red colors indicate velocity perturbations which are, respectively, higher and lower compared to the reference velocity model (Figure 6.1.12). Grey color indicates areas of poor ray coverage (less than 0.75 % of total ray hits). Dashed contours on the horizontal slice at 31.5 km depth and solid lines on vertical profiles mark the Moho intersection.

6.1.6 Conclusions

The main conclusions obtained from our study are as follows:

- The velocity perturbations vary ±0.4 km/s compared to the reference velocity model.
- The Moho boundary ranges from 31 km beneath the Oslo Graben and SW coast to about 35 km beneath the mountain plateau. However, the checkerboard test indicates relatively poor resolution below 35-40 km.
- The higher seismic velocities compared to the reference velocity model dominate under the mountain plateau.

I. Janutyte
T. Kværna

Appendix

Table 6.1.2 List of seismic events in Nordic format used to develop a velocity model for southern Norway. Notations: mmdd – month and day; ss.s – seconds, t – type of event at observation distance (L for local); latitu – latitude in degrees; longit - longitude in degrees; dept – depth in km; agg – reporting agency; st – number of stations with observations; res – location time residual in seconds; magTagg – magnitude, type of magnitude and the reporting agency.

Year	mmdd	hhmi	ss.s	t	latitu	longit	dept	agg	st	res	magTagg	magTagg	magTagg
2007	2	1	0211	26.1	L	57.063	7.120	10.4F	BER	26	0.2	1.7LBER	2.3CBER	1
2007	5	1	1411	30.1	L	57.644	10.572	0.0	BER	27	0.2	1.8LBER	2.3CBER	2.1LNAO1
2007	2	1	1426	8.7	L	61.177	6.904	0.0	BER	36	0.2	1.9LBER	1.6CBER	1.9LNAO1
2007	11	2	0818	3.3	L	62.852	5.844	15.9	TES	25	0.2	1.8LTES	2.2CTES	2.1WTES1
2007	10	2	1107	25.6	L	57.589	10.636	12.3	TES	30	0.2	1.8LTES	2.1WTES	1.9LNAO1
2007	10	2	1227	53.4	L	57.679	10.448	18.0	TES	24	0.2	1.7LTES	2.2WTES	1.8LNAO1
2007	10	2	1520	55.3	L	57.691	10.451	19.7	TES	25	0.2	1.7LTES	2.5CTES	2.2WTES1
2007	10	2	2000	3.8	L	57.703	10.460	17.0	TES	23	0.2	1.8LTES	2.2WTES	1.9LNAO1
2007	10	3	0959	37.0	L	57.666	10.424	5.3	TES	28	0.2	1.7LTES	2.6CTES	1.9LNAO1
2007	10	3	1235	19.9	L	57.735	10.430	21.4	TES	25	0.3	1.7LTES	2.4CTES	1.9LNAO1
2007	7	3	1425	1.9	L	58.163	8.313	30.1	BER	29	0.2	2.1LBER		2.0LNAO1
2007	10	3	2128	6.4	L	60.154	4.777	15.0	TES	42	0.3	2.1LTES	2.1WTES	2.0LNAO1
2007	5	4	0910	59.8	L	62.989	6.536	12.1	BER	44	0.3	2.2LBER	2.1CBER	2.2LNAO1
2007	7	4	1353	56.8	L	64.025	10.049	0.0F	BER	21	0.5	1.7LBER		2.1LNAO1
2007	7	4	1427	8.7	L	58.240	11.231	0.0	BER	16	0.2	1.4LBER		2.1LNAO1
2008	5	4	2257	23.9	L	62.525	4.095	12.1	TES	34	0.4	2.0LTES	2.4CTES	2.1WTES1
2007	12	5	1108	30.1	L	57.671	10.411	13.1	TES	13	0.4	1.6LTES	1.8WTES	1
2007	4	5	1736	7.6	L	60.621	4.628	16.1	BER	33	0.2	2.0LBER	1.7CBER	1.8LNAO1
2007	11	6	0907	59.0	L	59.662	7.399	14.7	TES	45	0.2	2.6LTES	2.6CTES	2.4LNAO1
2007	3	8	1055	42.1	L	64.015	9.735	0.0	BER	12	0.1	1.1LBER	2.5CBER	1
2007	12	8	1310	52.7	L	62.001	4.821	14.4	TES	12	0.2	1.2LTES	2.3CTES	1.4WTES1
2006	12	8	2240	13.8	L	57.477	7.160	15.0	BER	30	0.7	1.9LBER	1.0CBER	1
2008	4	9	1210	24.7	L	56.944	6.868	15.0	TES	26	0.3	2.1LTES	2.2WTES	1.8LNAO1
2008	4	9	1702	11.8	L	58.279	8.409	0.0	TES	23	0.3	1.5LTES	1.9WTES	1
2008	6	9	1900	7.0	L	62.202	5.571	12.1	TES	24	0.4	1.6LTES	1.7WTES	1
2006	1110	0854	20.0	L	60.938	10.128	26.0F	BER	20	0.1	1.5LBER	1.8WBER	1
2007	510	1341	13.8	L	61.803	5.104	4.7F	BER	39	0.1	2.1LBER	1.8CBER	1.8LNAO1
2007	110	2312	53.1	L	61.658	4.435	12.2	BER	46	0.5	2.5LBER	2.3CBER	2.2LNAO1
2007	111	1035	4.9	L	59.987	6.660	14.6	BER	30	0.2	1.9LBER	1.6CBER	2.0LNAO1
2006	1011	1200	25.3	L	61.784	5.193	1.5	BER	32	0.2	2.1LBER	1.5CBER	2.3WBER1
2008	612	1005	33.3	L	64.438	8.769	12.1	TES	10	0.1	1.9LTES	2.6CTES	1.9WTES1
2007	912	1413	42.9	L	59.038	9.862	2.6	BER	22	0.3	1.7LBER	2.2CBER	1
2008	212	1420	11.3	L	61.797	5.131	0.1	TES	25	0.3	1.8LTES	2.2WTES	2.0LNAO1
2007	1212	1427	15.8	L	59.024	9.888	0.0	TES	21	0.3	1.5LTES	1.7WTES	1
2008	612	1619	9.8	L	64.502	9.327	12.1	TES	6	0.4	1.3LTES		1

```
2007  912 2256 41.5 L  61.699   4.386 12.1  TES 50 0.3 2.9LTES 2.7WTES 2.8LNAO1
2007 1113 1731 20.0 L  63.088   7.814  9.6  TES  9 0.1 1.0LTES 1.5WTES        1
2007 1115 1432 36.2 L  58.826   6.071 12.2  TES 27 0.3 1.7LTES 1.9WTES        1
2007 1115 1514 27.8 L  58.966   9.916 12.1  TES 20 0.3 1.4LTES 1.6WTES        1
2008  615 2211  3.6 L  59.950   6.426  8.5  TES 31 0.3 1.7LTES 1.7WTES        1
2008  416 1453  7.5 L  61.404  11.540 12.1  TES 18 0.2 1.6LTES 2.2WTES 2.2LNAO1
2007  317 0006 27.0 L  59.702   6.715 12.1  BER 47 0.4 2.2LBER 1.9CBER 2.1LNAO1
2006 1117 1213 28.0 L  59.355   6.070  1.9  BER 19 0.2 1.2LBER 2.1CBER 1.3WBER1
2007  417 1216  0.1 L  61.785   5.177  0.0  BER 33 0.1 2.0LBER 1.4CBER 2.0LNAO1
2007  118 1205 27.7 L  59.983   4.624  1.2  BER 33 0.2 2.0LBER 1.9CBER 2.0LNAO1
2007  118 1213  3.7 L  59.973   4.712  0.0  BER 30 0.4 2.0LBER 1.5CBER 1.8LNAO1
2007  419 0419 29.5 L  64.008   9.713  1.0  BER 12 0.2 1.1LBER 2.2CBER        1
2007 1219 1333 52.6 L  57.511   7.272 12.6  TES 24 0.3 2.0LTES 2.2WTES        1
2006 1219 1740 40.8 L  61.315  11.586 22.4  BER 20 0.2 1.7LBER 2.1CBER 1.9WBER1
2007  920 1100 38.3 L  61.802   5.078  9.6  TES 18 0.2 1.8LTES 2.0WTES 2.0LNAO1
2006  920 1143 23.7 L  63.284   5.166 12.8  BER 21 0.3 1.9LBER 1.9CBER 2.0WBER1
2007  821 0153 47.3 L  58.251   7.883  2.4  BER 19 0.4 1.3LBER 2.0CBER        1
2007  121 1345 22.4 L  62.571   6.477  4.8  BER 48 0.3 3.6LBER 3.5CBER 3.8LNAO1
2007  521 2022 13.3 L  61.641   4.565  9.2  BER 42 0.1 2.3LBER 2.1CBER 2.1LNAO1
2007  622 0542  2.2 L  61.249   4.856  6.1  BER 39 0.2 1.9LBER 1.9CBER        1
2007  222 0722 20.3 L  62.756   7.009  9.0  BER 31 0.3 2.0LBER 1.9CBER 2.0LNAO1
2008  522 1259  2.2 L  61.787   5.043 12.2  TES 40 0.4 2.2LTES 2.5WTES 2.1LNAO1
2008  222 1321  4.9 L  61.792   5.076 12.2  TES 26 0.5 1.9LTES 1.8CTES 2.2WTES1
2008  122 1339  0.3 L  61.809   4.991 12.7  TES 34 0.5 2.0LTES 2.3WTES 2.1LNAO1
2008  424 0059 19.4 L  62.138   6.430 12.1  TES 35 0.2 1.7LTES 1.9WTES        1
2007  724 1224 41.2 L  61.777   5.225  3.5  BER 31 0.3 1.9LBER 1.7CBER        1
2007  524 1316 19.5 L  58.906   5.702  0.2  BER 14 0.1 1.4LBER                 1
2008  124 1851 51.3 L  57.488   7.272 12.1  TES 37 0.3 2.5LTES 2.4WTES 2.4LNAO1
2008  525 0110  5.6 L  60.097  10.718  7.6  TES 45 0.1 2.7LTES 3.0CTES 2.9LNAO1
2006  925 1244 57.4 L  57.542   7.269 17.2  BER 26 0.1 2.1LBER 1.9CBER 1.9LNAO1
2008  425 1522 46.4 L  59.036   9.879  1.1  TES 28 0.3 1.6LTES 1.8WTES        1
2008  425 1806  7.3 L  57.540  10.569 16.1  TES 34 0.4 1.9LTES 2.2WTES 2.1LNAO1
2007  627 1230 18.0 L  61.796   5.142  2.0  BER 39 0.1 2.0LBER 1.7CBER        1
2007  727 2330 22.2 L  61.832   4.545 18.9  BER 42 0.1 2.1LBER 2.0CBER 1.9LNAO1
2007  928 2156  8.3 L  56.961   6.923 30.4  TES 27 0.2 2.0LTES 2.2WTES 2.0LNAO1
2008  529 0828 49.5 L  62.623   4.894 12.8  TES 39 0.3 2.4LTES 2.3WTES 2.7LNAO1
2008  229 1308 28.4 L  61.382  11.562 12.1  TES 20 0.2 1.6LTES 2.1WTES 2.1LNAO1
2007  130 0834  5.5 L  61.381   4.073 12.4  BER 32 0.2 1.6LBER 1.9CBER 1.9WBER1
2007  530 1125 54.9 L  63.969   9.899  0.0  BER 27 0.2 2.0LBER                 1
2009  424 1837 10.5 L  60.162  10.883  0.0  EXP 13 1.2 2.0LEXP 2.7CEXP 2.2LNAO1
2009  6 7 1730 56.7 L  60.134   6.415  5.5  EXP 15 0.4 1.9LEXP 2.1CEXP 1.7LNAO1
2009  610 2247 46.4 L  61.223   7.202 15.0  EXP 11 0.6 1.5LEXP 2.1CEXP        1
2009 1030 0058 14.7 L  60.217  11.092 15.0  EXP 13 1.0 1.7LEXP 2.5CEXP 1.2LNAO1
2010  421 1752 29.0 L  61.032   7.713  0.4  EXP 11 0.5 1.0LEXP 1.9CEXP        1
2010  615 0422  3.8 L  60.829   6.784  0.0F EXP 15 0.8 1.5LEXP 2.2CEXP 2.1LNAO1
2010 10 8 0408 32.3 L  59.598   7.501 15.0F EXP 13 0.5 1.5LEXP 2.5CEXP 1.8LNAO1
2011  112 0601 53.7 L  60.238  10.509 15.0  EXP 24 0.6 1.8LEXP 2.2CEXP 1.9LNAO1
2011  327 1134 20.8 L  59.983  12.892 15.0  EXP 12 0.4 1.9LEXP 3.0CEXP 2.0LNAO1
2011  428 2224  6.6 L  59.938   6.782 12.0F EXP 16 0.5 2.0LEXP 2.3CEXP 2.0LNAO1
2011 1111 2049 55.9 L  59.857   6.451 12.1  EXP  9 0.3 1.0LEXP 2.1CEXP        1
2011 1223 1418 20.8 L  60.655   6.337 15.0  EXP  9 0.4 1.4LEXP 1.8CEXP        1
2012  124 1454 51.9 L  59.850   6.622 20.9  EXP 12 0.6 1.3LEXP                 1
2012  324 1106 30.8 L  60.598   6.353 15.0  EXP 51 1.0 3.0LEXP         3.2LNAO1
2012  328 1527 37.8 L  60.436   6.897  0.0  EXP 10 0.5 1.6LEXP                 1
2012  426 0518 28.9 L  60.065   7.255  0.0  EXP 26 0.5 1.9LEXP         1.9LNAO1
2012 1030 0357 26.9 L  61.250   6.539 13.4  EXP 13 0.5 1.4LEXP                 1
2013  2 5 1056  3.7 L  60.393   8.656  0.0  EXP 10 0.5 1.2LEXP                 1
2012 1127 1425 53.6 L  60.019  11.066  0.1  EXP 10 0.5 0.9LEXP                 1
2013  325 1448 24.9 L  59.666  12.609  0.0  EXP 11 0.5 1.1LEXP                 1
2013  415 1451 31.4 L  60.642   8.609  0.1  EXP 14 0.4 1.4LEXP                 1
2013  527 1206 25.4 L  59.934  10.544  0.0  EXP 11 0.4 1.3LEXP                 1
2013  613 1112  1.2 L  59.115   6.868  0.0  EXP  9 0.4 1.0LEXP                 1
2013  619 1831  5.1 L  61.212   6.985  0.0  EXP 20 0.5 1.4LEXP                 1
2013  626 1304  0.6 L  61.022   9.046  0.0  EXP 12 0.5 1.2LEXP                 1
2013  7 1 0911 17.2 L  61.018   8.182  4.3  EXP 10 0.5 1.1LEXP                 1
2013  7 4 1509 26.8 L  59.138   6.870  0.0  EXP 13 0.6 1.0LEXP                 1
2013  7 9 1040 42.1 L  60.025  11.052  0.0  EXP 11 0.5 1.2LEXP                 1
2013  723 1359 31.2 L  59.138   6.847  0.1  EXP 13 0.6 1.1LEXP                 1
2013  723 1648 50.7 L  60.956   9.363  0.0  EXP 26 0.4                 1.7LNAO1
2013  828 1443 23.6 L  60.718   9.031  0.0  EXP 14 0.4 1.3LEXP                 1
2013  9 3 1339 11.3 L  61.062   8.183 21.8  EXP 10 0.4 1.0LEXP                 1
2013  9 3 1715 32.2 L  60.738   9.001  0.0  EXP 12 0.4 1.0LEXP                 1
2013  911 1708 58.3 L  60.738   8.982  0.0  EXP 14 0.5 1.5LEXP                 1
2013  920 0127  0.7 L  60.043   6.735 17.3  EXP 26 0.6 2.4LEXP         2.4LNAO1
2013  926 1214 28.4 L  59.738  10.803  0.0  EXP 11 0.5 1.2LEXP                 1
2013 1016 1900  4.1 L  60.063   9.135  0.1  EXP 12 0.4 0.8LEXP                 1
2013 1022 1221  1.1 L  60.025   9.273  0.0  EXP 13 0.4 1.3LEXP                 1
```

```
2013 1024 1213 52.3 L  60.313   9.005  0.1  EXP  9 0.4 1.3LEXP                1
2013 1113 1544 16.6 L  60.578   8.394  0.0  EXP 16 0.4 1.4LEXP                1
2013 1119 2341  8.2 L  61.490   7.152 14.0F EXP 36 0.6 2.9LEXP 2.9WEXP 2.7LNAO1
2013 12 3 1612 44.3 L  60.652   8.576  8.6  EXP 11 0.2 1.3LEXP                1
2013 12 5 1158  3.6 L  60.950   9.331  0.0  EXP 21 0.2 1.4LEXP         1.7LNAO1
2013 1210 1256  5.9 L  60.598   8.552  0.0  EXP 10 0.3 1.2LEXP                1
2013 1210 1735 12.2 L  60.474   9.202  0.0  EXP 16 0.4 1.5LEXP                1
2013 1211 1505  8.1 L  60.481   8.544  0.0  EXP 13 0.3 1.1LEXP                1
2013 1217 0945 23.3 L  60.274   8.979 11.4  EXP 10 0.3 1.0LEXP                1
2013 1219 1404 31.9 L  60.450   9.202  0.1  EXP 13 0.4 1.2LEXP                1
2014 0108 2048 11.8 L  61.568   3.141  6.4  NAO 11 0.8                 1.6LNAO1
2014 0115 1934 55.9 L  60.430   7.143       NAO 17 0.9                 2.1LNAO1
2014 0118 1425 10.6 L  60.045   6.546       NAO 16 0.6                 2.0LNAO1
2014 0119 0644 24.4 L  59.984   6.434  6.3  NAO  9 1.1                 1.6LNAO1
2014 0121 0639 03.4 L  61.053   4.717 13.6  NAO 14 1.3                 2.4LNAO1
2014 0123 0432 49.7 L  61.243   4.790  9.6  NAO 19 1.2                 2.6LNAO1
2014 0220 1320 47.2 L  61.753   5.319       NAO  7 1.1                 2.0LNAO1
2014 0224 1339 20.2 L  58.299  10.974       NAO  9 1.0                 2.1LNAO1
2014 0227 1502 19.4 L  60.831   5.381  4.4  NAO  9 0.9                 1.9LNAO1
2014 0308 1038 20.3 L  61.455   4.575 12.5  NAO  9 1.4                 1.9LNAO1
2014 0401 0947 25.9 L  59.357  10.480       NAO 17 0.8                    LNAO1
2014 0401 1235 29.5 L  59.442  10.498       NAO 15 1.2                    LNAO1
2014 0402 0737 02.1 L  59.394  10.478       NAO 13 1.1                 1.7LNAO1
2014 0402 0812 50.0 L  59.366  10.481       NAO 16 0.8                 1.8LNAO1
2014 0402 1044 54.5 L  59.413  10.493       NAO 14 0.8                 2.1LNAO1
2014 0402 1107 24.2 L  59.814  10.556       NAO 15 0.8                 1.8LNAO1
2014 0402 1226 01.7 L  59.419  10.484       NAO 16 0.9                 2.4LNAO1
2014 0402 1308 44.7 L  60.707   5.695       NAO  7 1.0                 1.6LNAO1
2014 0402 1432 15.4 L  59.877  10.538       NAO 15 1.1                 2.3LNAO1
2014 0402 1635 10.0 L  59.832  10.545       NAO 14 0.9                 1.7LNAO1
2014 0404 2330 48.6 L  59.963   5.920       NAO  6 0.7                 1.8LNAO1
2014 0408 0650 12.3 L  62.322   3.625  1.8  NAO 16 0.8                 2.7LNAO1
2014 0503 1724 20.2 L  59.526   6.240 21.9  NAO  9 1.0                 1.7LNAO1
2014 0505 1334 48.1 L  62.288   6.101 18.4  NAO  7 1.5                 2.4LNAO1
2014 0512 1604 46.1 L  61.739   5.338       NAO  8 1.1                 2.0LNAO1
2014 0523 1318 51.2 L  58.528   6.321       NAO  4 1.5                 1.7LNAO1
2014 0616 1231 04.7 L  60.689   5.652       NAO  6 0.9                 1.9LNAO1
2014 0623 1100 52.8 L  60.692   5.646       NAO  8 1.2                 1.7LNAO1
2014 0626 0131 15.5 L  61.911   5.619       NAO  8 1.1                 1.9LNAO1
2014 0702 0528 28.0 L  62.064   3.069  4.5  NAO  7 1.4                 1.8LNAO1
2014 0705 1334 30.5 L  61.666   4.303 11.9  NAO  8 0.7                 2.0LNAO1
2014  9 6 1656 38.1 L  59.942   6.347  0.2  BER 24 0.4 2.4LBER                1
2007 1001 1939 52.0 L  62.568 007.733  0.0F                                   1
2007 1001 1950 05.0 L  61.293 010.123  0.0F                                   1
2007 1001 2000 06.6 L  62.948 007.390  0.0F                                   1
2007 1001 2009 52.7 L  61.751 009.515  0.0F                                   1
2007 1001 2020 00.0 L  59.242 012.984  0.0F                                   1
2007 1001 2030 19.5 L  63.053 010.265  0.0F                                   1
2007 1001 2040 14.9 L  62.627 009.809  0.0F                                   1
2007 1001 2051 24.8 L  62.461 009.546  0.0F                                   1
2007 1001 2101 03.3 L  61.209 007.163  0.0F                                   1
2007 1001 2110 01.2 L  60.848 006.733  0.0F                                   1
2007 1001 2120 04.7 L  61.074 010.511  0.0F                                   1
2007 1001 2129 59.9 L  62.233 008.223  0.0F                                   1
2007 1001 2340 01.7 L  59.630 009.010  0.0F                                   1
2007 1002 0400 02.2 L  59.657 007.990  0.0F                                   1
2007 1002 1949 53.1 L  61.482 010.183  0.0F                                   1
2007 1002 2009 57.6 L  60.675 011.223  0.0F                                   1
2007 1002 2019 47.4 L  62.789 010.020  0.0F                                   1
2007 1002 2030 00.9 L  61.939 009.168  0.0F                                   1
2007 1002 2040 00.4 L  61.663 008.183  0.0F                                   1
2007 1002 2050 00.8 L  60.652 006.504  0.0F                                   1
2007 1002 2210 03.9 L  59.581 011.363  0.0F                                   1
2007 1002 2230 02.7 L  59.525 005.698  0.0F                                   1
2007 1003 0150 00.9 L  59.363 012.481  0.0F                                   1
2007 1003 0210 05.0 L  59.573 010.167  0.0F                                   1
```

References

Andersen, T.B. (1998). Extensional tectonics in the Caledonides of southern Norway, and overview. *Tectonophysics*, 285, 333–351.

Balling, N. (1980). The land uplift of Fennoscandia, gravity field anomalies and isostasy. In *Earth Rheology, Isostasy and Eustasy* (ed. Mørner, N.A.), John Wiley & Sons, New York, pp. 297–321.

Faleide, J.I., Kyrkjebø, R., Kjennerud, T., Gabrielsen, R.H., Jordt, H., Fanavoll, S. and M.D. Bjerke (2002). Tectonic impact on sedimentary processes during the Cainozoic evolution of the northern North Sea and surrounding areas. *Geol. Soc. London Spec. Publication*, Vol. 196.

Kissling, E. (1995). Program VELEST user's guide – Short introduction. Institute of Geophysics, ETH Zurich, Second draft version 5th October, 1995.

Kolstrup, M.L. (2015). Old structures and plumes? – New geophysical investigations of the crust and upper mantle in southwestern Scandinavia. Doctoral dissertation, University of Oslo, Faculty of Mathematics and Natural Sciences, Department of Geosciences, ISSN 1501-7710, Nr. 1615, pp.147.

Lidmar-Bergstrøm, K., Ollier, C.D. and J.R. Sulebak (2000). Landforms and uplift history of southern Norway. *Global Planet. Change*, 24, 211–231.

Ottemoller, L., Voss, P.H. and J. Havskov (2014). SEISAN EARTHQUAKE ANALYSIS SOFTWARE FOR WINDOWS, SOLARIS, LINUX and MACOSX , 2014.

Rawlinson, N., and M. Sambridge (2005). The fast marching method: an effective tool for tomographic imaging and tracking multiple phases in complex layered media. *Exploration Geophysics* 36 (4), 341-350.

Roberts, D. and D.G. Gee (1985). An introduction to the structure of the Scandinavian Caledonide Orogen. John Wiley & Sons, Chichester.

Sellevoll, M.A. and R.E. Warrick (1971). A refraction study of the crustal structure in southern Norway. *Bull. seism. Soc. Am*., 61, 457–471.

Stratford, W., Thybo, H., Faleide, J.I., Olesen, O., and A. Tryggvason (2009). New Moho Map for onshore southern Norway. *Geophys. J. Int*, 178, 1755–1765.

Stratford, W. R., and H. Thybo (2011). Seismic structure and composition of the crust beneath the southern Scandes, Norway. *Tectonophysics*, Vol. 502, No. 3-4, p. 364-382.